HHS Public Access

Author manuscript

Biochem Pharmacol. Author manuscript; available in PMC 2021 October 01.

Published in final edited form as:

Biochem Pharmacol. 2020 October ; 180: 114137. doi:10.1016/j.bcp.2020.114137.

Overexpression of ABCB1 and ABCG2 contributes to reduced efficacy of the PI3K/mTOR inhibitor samotolisib (LY3023414) in cancer cell lines

Chung-Pu Wu[a,b,c,f,*], **Cheng-Yu Hung**[c], **Sabrina Lusvarghi**[h], **Yang-Hui Huang**[b], **Pin-Jung Tseng**[a], **Tai-Ho Hung**[e,f], **Jau-Song Yu**[a,c,d,g], **Suresh. V. Ambudkar**[h]

[a]Graduate Institute of Biomedical Sciences, Chang Gung University, Tao-Yuan, Taiwan.

[b]Department of Physiology and Pharmacology, Chang Gung University, Tao-Yuan, Taiwan.

[c]Molecular Medicine Research Center, Chang Gung University, Tao-Yuan, Taiwan.

[d]Department of Biochemistry and Molecular Biology, Chang Gung University, Tao-Yuan, Taiwan.

[e]Department of Chinese Medicine, College of Medicine, Chang Gung University, Tao-Yuan, Taiwan.

[f]Department of Obstetrics and Gynecology, Taipei Chang Gung Memorial Hospital, Taipei, Taiwan.

[g]Liver Research Center, Chang Gung Memorial Hospital, Linkou, Taiwan.

[h]Laboratory of Cell Biology, Center for Cancer Research, National Cancer Institute, NIH, Bethesda, MD, United States.

Abstract

LY3023414 (samotolisib) is a promising new dual inhibitor of phosphoinositide 3-kinase (PI3K) and mammalian target of rapamycin (mTOR). Currently, multiple clinical trials are underway to evaluate the efficacy of LY3023414 in patients with various types of cancer. However, the potential mechanisms underlying acquired resistance to LY3023414 in human cancer cells still remain elusive. In this study, we investigated whether the overexpression of ATP-binding cassette (ABC) drug transporters such as ABCB1 and ABCG2, one of the most common mechanisms for developing multidrug resistance, may potentially reduce the efficacy of LY3023414 in human cancer cells. We demonstrated that the intracellular accumulation of LY3023414 in cancer cells was significantly reduced by the drug efflux function of ABCB1 and ABCG2. Consequently, the cytotoxicity and efficacy of LY3023414 for inhibiting the activation of the PI3K pathway and induction of G0/G1 cell-cycle arrest were substantially reduced in cancer cells overexpressing

[*]Corresponding author at: 259 Wen-Hwa 1st Road, Kwei-Shan, Tao-Yuan 333, Taiwan. Phone: +886-3-2118800, ext. 3754. Fax: +886-3-2118700. wuchung@mail.cgu.edu.tw.

5. Conflict of interest

The authors declare no conflict of interest.

ABCB1 or ABCG2, which could be restored using tariquidar or Ko143, respectively. Furthermore, stimulatory effect of LY3023414 on the ATPase activity of ABCB1 and ABCG2, as well as *in silico* molecular docking analysis of LY3023414 binding to the substrate-binding pockets of these transporters provided additional insight into the manner in which LY3023414 interacts with both transporters. In conclusion, we report that LY3023414 is a substrate for ABCB1 and ABCG2 transporters implicating their role in the development of resistance to LY3023414, which can have substantial clinical implications and should be further investigated.

Graphical Abstract

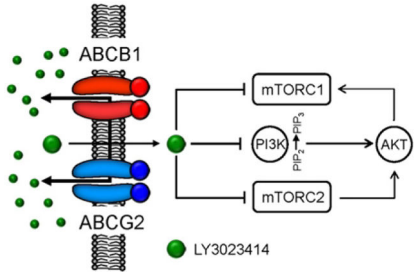

Keywords

ABCB1; ABCG2; Multidrug resistance; PI3K/mTOR; LY3023414

1. Introduction

The PI3K-AKT-mTOR (PAM) pathway is a key regulatory signaling pathway that is crucial for cell proliferation, metabolism, and survival. Studies have demonstrated that through various molecular alterations, constitutive activation of this pathway is frequent in human cancer [1]. In addition, alterations of the PAM signaling pathway is often implicated in acquired drug resistance in human cancer [2–5]. More importantly, studies have found that many of these alterations in the PAM pathway are druggable, and direct inhibition can lead to regression of human tumors, resulting in the accelerated development of novel PAM inhibitors [1, 6]. Notably, PAM inhibitors such as idelalisib, copanlisib, alpelisib, everolimus, and temsirolimus have already been approved by the U.S. Food and Drug Administration (FDA) for the treatment of different types of cancer [7, 8], and many novel inhibitors are currently under clinical investigation.

LY3023414, also known as samotolisib, is a promising new PI3K/mTOR dual inhibitor that is currently being tested in clinical trials for the treatment of triple-negative breast cancer (ClinicalTrials.gov Identifier: NCT04032080), metastatic breast cancer (NCT02057133), endometrial cancer (NCT02549989), prostate cancer (NCT02407054), Non-Hodgkin lymphoma (NCT03213678), non-small cell lung cancer (NSCLC) (NCT02079636), pancreatic ductal adenocarcinoma (NCT02981342), and advanced cancers (NCT02784795, NCT02536586, NCT03155620, NCT02124148, and NCT01655225). However, the potential mechanisms underlying acquired resistance to LY3023414 in human cancer cells have not been investigated. Along with the most common mechanisms of resistance to PAM

inhibitors [9], such as extensive crosstalk between the PAM pathway and other key signaling pathways [5], drug efflux pumps such as ABCB1 (P-glycoprotein, MDR1) and ABCG2 (BCRP, MXR) can potentially reduce the efficacy of LY3023414 in human cancer cells. ABCB1 and ABCG2 are members of the ATP-Binding Cassette (ABC) transporter superfamily that are infamous for reducing the chemosensitivity of cancer cells to conventional anticancer drugs. By utilizing energy derived from ATP hydrolysis, these drug transporters can actively efflux a wide variety of cytotoxic anticancer drugs out of cancer cells and away from their intracellular targets [10, 11]. As a result, the overexpression of ABCB1 and/or ABCG2 often contributes to the development of multidrug resistance (MDR) phenotype in human cancer cells, resulting in treatment failure and relapse [10, 12, 13]. Moreover, as an endogenous defense mechanism against xenobiotics, ABCB1 and ABCG2 are highly expressed in the small intestine, liver, and kidney, as well as blood-tissue barriers, such as the blood-brain barrier (BBB), the blood-testis barrier (BTB), and the placental barrier [14]. Collectively, ABCB1 and ABCG2 can significantly alter the pharmacokinetics of most therapeutic drugs [15, 16]. It is worth noting that recent studies have demonstrated that the drug efflux function of ABCB1 and ABCG2 significantly limits the bioavailability, distribution and the efficacy of many molecularly targeted therapeutic agents, including, but not limited to, epidermal growth factor receptor (EGFR) inhibitors [17–19], vascular endothelial growth factor receptor (VEGFR) inhibitors [20], rapidly accelerated fibrosarcoma (RAF) inhibitors [21–24], PARP inhibitors [25–27], as well as PI3K [28–30] and mTOR inhibitors [31–33].

In this study, we examined the role of ABCB1 and/or ABCG2 for the development of resistance or reduced susceptibility of cancer cells to LY3023414. We discovered that the intracellular accumulation, the efficacy, and cytotoxicity of LY3023414 are significantly reduced in cancer cells overexpressing ABCB1 or ABCG2, which can be restored by inhibiting the function of ABCB1 and ABCG2. The results of this study indicate that the overexpression of ABCB1 or ABCG2 may be a contributing factor to LY3023414 resistance, and drug combination therapy with a modulator of ABCB1 and ABCG2 may be required to achieve a better clinical outcome.

2. Materials and methods

2.1. Chemicals

RPMI medium, Iscove's Modified Dulbecco's medium (IMDM), Dulbecco's Modified Eagle's medium (DMEM), phosphate-buffered saline (PBS), Fetal calf serum (FCS), trypsin-EDTA, penicillin and streptomycin were purchased from Gibco, Invitrogen (CA, USA). Tools Cell Counting (CCK-8) Kit was purchased from Biotools Co., Ltd (Taipei, Taiwan). LY3023414 (samotolisib) was purchased from Selleckchem (Houston, TX, USA). Annexin V: FITC Apoptosis Detection Kit was purchased from BD Pharmingen (San Diego, CA, USA). MTT dye and all other chemicals were purchased from Sigma-Aldrich (St. Louis, MO, USA) unless stated otherwise.

2.2. Cell lines and culture conditions

The human ovarian cancer OVCAR-8 and NCI-ADR-RES cell line pair [34]; the human epidermal cancer KB-3–1 and KB-V-1 cell line pair [35]; HEK293 cells stably transfected with either empty pcDNA 3.1 vector (pcDNA3.1-HEK293), HEK293 stably transfected with human ABCB1 (HEK293 cells stably expressing ABCB1 are referred in this manuscript as MDR19-HEK293) [36] or human ABCG2 (HEK293 cells stably expressing ABCG2, 482R-HEK293, clone 5, are referred in this manuscript as R482-HEK293) [37] were maintained in DMEM supplemented with 10% FCS, 2 mM L-glutamine and 100 units of penicillin/streptomycin/mL. The human colon cancer S1 and S1-M1-80 cell line pair [38]; the human non-small cell lung cancer H460 and H460-MX20 cell line pair [39], were maintained in RPMI-1640 supplemented with 10% FCS, 2 mM L-glutamine and 100 units of penicillin/streptomycin/mL. The KB-V-1 cell line, NCI-ADR-RES cell line, S1-M1-80 cell line and H460-MX20 were maintained in media containing 1 mg/mL vinblastine [40], 0.85 μM doxorubicin [34], 80 μM of mitoxantrone [38] or 20 nM of mitoxantrone [41], respectively. The HEK293 and HEK293 transfected lines were maintained in 2 mg/mL G418, as described previously [42]. The OVCAR-8, NCI-ADR-RES, KB-3–1 and KB-V-1 cell lines were generous gift from Dr. Michael Gottesman (NCI, NIH, Bethesda, MD, USA), whereas the H460, H460-MX20, S1, S1-M1-80, HEK293 and HEK293 transfected lines were generous gift from Dr. Susan Bates (NCI, NIH, Bethesda, MD, USA). All cell lines were cultured at 37 °C in 5% CO_2 humidified air and placed in drug-free medium 7 days prior to assay.

2.3. Cytotoxicity assay

The cytotoxicity of LY3023414 in various cell lines was determined by cytotoxic (MTT and CCK-8) assays as previously described [43]. Briefly, cells were seeded at a density of 5000 cells per well in 96-well plates and cultured in the medium at 37 °C for 24 h. Cells were subsequently treated with LY3023414 in the absence or presence of 1 μM tariquidar or Ko143 with 0.5% (v/v) final concentration of DMSO in all wells for an additional 72 h and developed as described previously [44].

2.4. Immunoblotting

Membranes were incubated with anti-phospho-Akt (Thr308)(244F9) (#4056, Cell Signaling Technology, Danvers, MA, USA), anti-phospho-Akt (Ser473) (#9271, Cell Signaling Technology, Danvers, MA, USA), Akt1/2 Antibody (N-19) (#Sc-1619, Santa Cruz Biotechnology, Santa Cruz, CA, USA), Phospho-p70 S6 Kinase (Thr389)(108D2) (#9234, Cell Signaling Technology, Danvers, MA, USA), p70 S6 Kinase (#9202, Cell Signaling Technology, Danvers, MA, USA), phospho-S6 Ribosomal Protein (Ser240/244) (D68F8) (#5364, Cell Signaling Technology, Danvers, MA, USA), S6 Ribosomal Protein (5G10) (#2217, Cell Signaling Technology, Danvers, MA, USA), anti-P-glycoprotein C219 (#517310, Merck Millipore, Burlington, MA, USA), anti-BCRP/ABCG2 antibody BXP-21 (#ab3380, Abcam, Cambridge, MA, USA), or anti-α-tubulin (#T6199, Sigma-Aldrich, St. Louis, MO, USA) primary antibody and subsequently incubated with horseradish peroxidase-conjugated goat anti-mouse immunoglobulin G (IgG) or anti-rabbit IgG secondary antibodies. Signals were detected as described previously [44].

2.5. Cell Cycle Analysis

The standard propidium iodide (PI) staining method and a FACSort flow cytometer equipped with CellQuest software were used to analyze cell-cycle experiments as described previously [45]. Briefly, cells were treated with DMSO (control), 2 μM of LY3023414, 1 μM of tariquidar, 1 μM of Ko143, or in combination regimens as indicated for 24 h before harvested in PBS and fixed in ethanol overnight. Cells were washed once with PBS, then treated with 0.5 % TritonX-100 and 0.05 % RNase in PBS at 37 °C for 1 h. After washing cells with PBS, PI (50 μg/mL) was added and incubated at 4 °C for at least 20 min before analysis.

2.6. LC-MS/MS analysis of LY3023414 in cancer cells

LC-MS/MS conditions for determining the intracellular concentration of LY3023414 was performed and quantified according to the method described previously [29, 46] with slight modification. Briefly, 2×10^6 cells were maintained in 10 μM of LY3023414 in the absence or presence of 10 μM of tariquidar or Ko143 at 37 °C for 1 h, washed twice with cold PBS, harvested, and resuspended in three volumes of methanol and stored at −20 °C overnight. Cell lysates with methanol extraction were thawed and spun down (500×g) at 4 °C for 30 min. Supernatants were dried using the speed-vacuum-drying system and reconstituted in 50% methanol/H_2O and 0.1% formic acid. The analysis was performed using the Waters ACQUITY UPLC (ultra-performance liquid chromatography) system with a Waters BEH C18 Column (130Å, 1.7 μm, 1 × 100 mm) coupled with HCT ultra (Bruker Daltonik GmbH, Bremen, Germany) by the Selected Reaction Monitoring (SRM) in positive mode. The mobile phase: A = 0.1% formic acid in water and B = 0.1% formic acid in acetonitrile. The gradient method: 0 min, 20% B; 4.5 min, 20% B; 5 min, 95% B; 6.8 min, 20% B; 10 min, 20% B. A flow rate was 60 μL/min with a constant column temperature of 40°C. The SRM transition for LY3023414 (precursor ion m/z 407.5, fragment ion m/z 335.2) was integrated using DataAnalysis 4.2 software (Bruker Corporation, MA, USA), and the MS2 fragment 335.2 was calculated for quantitation by their peak areas. The internal standard was prepared from LY3023414 stock by serial dilution, and the equal matrix background of cell extraction was added to construct the calibration curve of the LY3023414 for LC-SRM/MS analysis. This calibration curve was subsequently used to quantify the intracellular accumulation of LY3023414 in OVCAR-8, NCI-ADR-RES, S1 and S1-M1-80 cells after treatment with LY3023414 in the presence or absence of tariquidar or Ko143. The standard response curve for LY3023414 was generated using cell lysate extracts as background, ranging from 50 nM to 50 μM.

2.7. Fluorescent drug accumulation assay

The accumulation of fluorescent calcein-AM (485 nm excitation and 535 nm emission) or Pheophorbide A (PhA) (395 nm excitation and 670 nm emission) in cancer cells were measured according to the method described by Gribar *et al.* [47]. Briefly, cells were first trypsinized and resuspended in IMDM containing 5% FCS before calcein or PhA was added to 3×10^5 cells in 4 mL of IMDM in the presence of DMSO (control), LY3023414, tariquidar or Ko143. The relative fluorescence intensity was determined using a FACSort

flow cytometer equipped with Cell Quest software (Becton-Dickinson) as described previously [48].

2.8. ATPase assay

The effect of LY3023414 on vanadate (V_i)-sensitive ATPase activity of ABCB1 or ABCG2 in membrane vesicles of High-Five cells expressing ABCB1 or ABCG2 was recorded by endpoint P_i assay as described previously [49]. Briefly, membrane vesicles from High-Five insect cells (Thermo Fisher Scientific, Waltman, MA, USA) infected with recombinant baculovirus containing ABCB1 or ABCG2 genes were prepared by hypotonic lysis followed by differential centrifugation [50, 51] as described previously [52]. Membrane vesicles (5 μg total protein) were incubated in the absence or presence of 0.3 mM sodium orthovanadate in ATPase buffer containing 50 mM MES-Tris pH 6.8, 1 mM EGTA, 5 mM NaN_3, 2 mM DTT, 50 mM KCl and 1 mM ouabain. Increasing concentrations of LY3023414 in DMSO or 1% DMSO were added to the ATPase reaction mixture and samples were incubated for 3 min at 37°C. ATP (5 mM) was added to start the ATP hydrolysis reaction, and the reaction was stopped after 20 min by the addition of 50 μL of P_i reagent containing 1% ammonium molybdate in 2.5 N H_2SO_4 and 0.014 % antimony potassium tartrate. Sodium L-ascorbate (0.33%, 100 μL) was added to the reaction mixture and the absorbance (880 nm) was measured after 10 min using a Spectramax® (Molecular Devices, San Jose, CA, USA) to quantify the amount of inorganic phosphate liberated during the reaction. The V_i-sensitive activity was calculated by subtracting the activity in the presence of vanadate from the total ATPase activity, as described previously [49].

2.9. Docking of LY3023414 in the drug-binding pocket of human ABCB1 and ABCG2

AutoDock Vina [53] was used as a docking software for docking of LY3023414 with the structures of the inward-open conformation of human ABCB1 (PDBID:6QEX) [54] and ABCG2 (PDBID:5NJ3) [55] as previously described [56]. MGLtools software package (Scripps Research Institute) was used to prepare the pdbqt files. For docking in the drug-binding pocket of ABCB1, the following residues were set as flexible: L65, M68, M69, F72, Q195, W232, F303, I306, Y307, Y310, F314, F336, L339, I340, F343, Q347, N721, Q725, F728, F732, F759, F770, F938, F942, Q946, M949, Y953, F957, L975, F978, V982, F983, M986, Q990, F993, F994, these 36 residues are all located in the drug-binding pocket in the transmembrane region of ABCB1. The receptor grid was centered at x = 19, y = 53, and z = 3, and a box with inner box dimensions 40 Å × 40 Å × 44 Å was used to search for all the possible binding poses within the transmembrane region of the protein. In the case of ABCG2, N393, A397, N398, V401, L405, I409, T413, N424, F431, F432, T435, N436, F439, S440, V442, S443, Y538, L539, T542, I543, V546, F547, M549, I550, L554, L555 from each monomer were set as flexible. The receptor grid centered at x = 125, y = 125, and z = 130 and a box with inner box dimensions 40 Å × 30 Å × 50 Å was used. The exhaustiveness level for both proteins was set at 100 to ensure that the global minimum of the scoring function would be found considering the large box size and the number of flexible residues. PyMOL molecular graphics system, Version 1.7, Shrödinger, LLC, was used for the visualization and analysis of both transporters and ligands.

2.10. Quantification and statistical analysis

The experimental data are presented as mean ± standard deviation (SD) calculated from at least three independent experiments. In the determination of cytotoxicity, the values are given as mean ± standard error of the mean (SEM). KaleidaGraph (Synergy Software, Reading, PA, USA) and GraphPad Prism (GraphPad Software, La Jolla, CA, USA) software were used for statistical analysis and curve plotting. The difference between mean values of experimental and control or improvement in fit was analyzed by two-sided Student's t-test and labeled with asterisks as "statistically significant" if the probability, p, was less than 0.05.

3. Results

3.1. LY3023414 is less cytotoxic in cells overexpressing ABCB1 or ABCG2

To determine the impact of ABCB1 and ABCG2 on the antiproliferative effect of LY3023414, we examined the cytotoxicity of LY3023414 in multiple pairs of drug-sensitive cell lines and multidrug-resistant variants overexpressing ABCB1 or ABCG2. We discovered that the drug-sensitive parental human OVCAR-8 ovarian cancer cells and the human KB-3–1 epidermal cancer cells were considerably more sensitive to LY3023414 than their respective ABCB1-overexpressing variants NCI-ADR-RES (Fig. 1A) and KB-V-1 (Fig. 1B). Moreover, the drug-sensitive parental human S1 colon cancer cells and the human H460 lung cancer cells were also more sensitive to LY3023414 than their respective ABCG2-overexpressing variant S1-M1-80 (Fig. 1C) and H460-MX20 (Fig. 1D). To confirm our findings, the cytotoxicity of LY3023414 was determined in HEK293 and HEK293 cells transfected with human ABCB1 (MDR19-HEK293) or human ABCG2 (R482-HEK293) to demonstrate that LY3023414 resistance was mediated by ABCB1 and ABCG2 (Fig. 1E). The IC_{50} and the resistance factor (RF) values for LY3023414 in these cell lines are summarized in Table 1. The RF value here represents the extent of cellular resistance to LY3023414 mediated by ABCB1 or ABCG2, which was calculated by dividing the IC_{50} value for LY3023414 in a drug-resistant variant by the value in the corresponding parental line. The calculated RF values ranged from approximately 8 to 37 for ABCB1 and approximately 12 to 41 for ABCG2 (Table 1). It is apparent that LY3023414 is significantly less cytotoxic in cancer cells expressing ABCB1 or ABCG2, regardless of tissue of origin. More importantly, we found that the antiproliferative effect of LY3023414 was fully restored by inhibiting the function of ABCB1 and ABCG2 in cells expressing ABCB1 or ABCG2, respectively (Table 2). Tariquidar, a reference inhibitor for ABCB1, resensitized NCI-ADR-RES cells and MDR19-HEK293 cells to LY3023414 by approximately 6-fold and 8-fold, whereas Ko143, a reference inhibitor for ABCG2, resensitized S1-M1-80 cells and R482-HEK293 cells to LY3023414 by approximately 8-fold and 7-fold. Our results suggest that the drug efflux function of ABCB1 and ABCG2 contributes directly to LY3023414 resistance in cancer cells.

3.2. The activity of LY3023414 on the phosphorylation status of PI3K/AKT/mTOR pathway kinases is reduced in cancer cells overexpressing ABCB1 or ABCG2

Previous studies have reported that treating cells with LY3023414 leads to the inhibition of PI3K/AKT/mTOR signaling and induction of cell-cycle arrest in cancer cells [57–59]. To

this end, we evaluated the effect LY3023414 in drug-sensitive OVCAR-8 and S1 cancer cells, as well as in the corresponding drug-resistant lines NCI-ADR-RES and S1-M1-80. Of note, cancer cell lines with the lowest RF values were used in these experiments to avoid overstating the effect of ABCB1 and ABCG2 on LY3023414. Cells were treated with increasing concentrations (0 – 10 μM) of LY3023414 for 2 h, and the effect of LY3023414 on the phosphorylation of PI3K downstream molecules was determined as described by Smith *et al.* [57]. As expected, phosphorylation of AKT at both threonine 308 (pT308 AKT) and serine 473 (pS473 AKT) was inhibited by LY3023414 in a concentration-dependent manner in all the cell lines tested (Fig. 2A). Moreover, the phosphorylation of S6 ribosomal protein (pS240/244 S6RP), a downstream target of the PI3K/AKT/mTOR pathway, was also inhibited by LY3023414. However, we noticed that the inhibition of phosphorylation of AKT by LY3023414 was less effective in ABCB1-overexpressing NCI-ADR-RES and ABCG2-overexpressing S1-M1-80 cancer cells as compared to their respective parental OVCAR-8 and S1 cells (Fig. 2A). As a result, we examine whether tariquidar and Ko143 could restore the activity of LY3023414 on pT308 AKT and pS473 AKT in NCI-ADR-RES and S1-M1-80 cancer cells. Cells were treated with DMSO (control), LY3023414 at 2 μM, GDC-0980 at 10 μM, tariquidar at1 μM, or Ko143 at 1 μM alone or in combination as indicated. We discovered that without affecting total AKT (t-AKT) or total S6RP (t-S6), tariquidar and Ko143 significantly increased the inhibition of pT308 AKT and pS473 AKT by LY3023414 in NCI-ADR-RES (Fig. 2B) and S1-M1-80 (Fig. 2C) cancer cells, respectively. Notably, a high concentration of the PI3K/mTOR kinase inhibitor GDC-0980 [60] was used as a positive control. Moreover, tariquidar or Ko143 alone did not affect the phosphorylation of AKT (pT308 AKT and pS473 AKT) or S6RP (p-S6) in these cell lines.

Next, we examined the effect of ABCB1 and ABCG2 on LY3023414-induced cell-cycle arrest in cancer cell lines. As expected, 2 μM of LY3023414 substantially induced G0/G1 cell-cycle arrest in OVCAR-8 (from 42 % basal level to 55 %) and S1 (from 51 % basal level to 74 %) cancer cells. In contrast, LY3023414 had a minor effect on G0/G1 cell-cycle arrest in ABCB1-overexpressing NCI-ADR-RES cancer cells or ABCG2-overexpressing S1-M1-80 cancer cells (Fig. 2D). More importantly, tariquidar and Ko143 (1 μM) significantly increased G0/G1 cell-cycle arrest induced by LY3023414 in NCI-ADR-RES (from 52 % basal level to 72 %) and S1-M1-80 (from 54 % basal level to 66 %) cancer cells. Of note, tariquidar or Ko143 alone had no significant effect on G0/G1 cell-cycle arrest in all tested cell lines. Together, our results indicate that the drug transport function of ABCB1 and ABCG2 reduces the efficacy of LY3023414 in cancer cells.

3.3. Overexpression of ABCB1 or ABCG2 reduces the intracellular accumulation of LY3023414 in cancer cells

One of the most probable causes for the lack of chemosensitivity attributable to the activity of ABCB1 and ABCG2 is reduced drug accumulation in cancer cells. To this end, we examined the intracellular accumulation of LY3023414 in OVCAR-8 and its ABCB1-overexpressing variant NCI-ADR-RES cancer cell lines, as well as in S1 and its ABCG2-overexpressing variant S1-M1-80 cancer cell lines, in the absence or presence of tariquidar or Ko143 using LC-MS/MS (Fig. 3A) as described previously [29, 46]. As shown in Fig. 3B, the intracellular accumulation of LY3023414 in NCI-ADR-RES and S1-M1-80 cancer cells

was significantly lower than in parental OVCAR-8 (1.84 ± 0.25 pmole/μL) and S1 (2.34 ± 0.54 pmole/μL) cancer cells, which could be restored by tariquidar and Ko143, respectively.

3.4. LY3023414 attenuates ABCB1- and ABCG2-mediated drug efflux

ABCB1- and ABCG2-mediated transport of one drug substrate usually interferes with the transport of another drug substrate [42, 61–63]. To this end, we examined the effect of LY3023414 on ABCB1-mediated transport of calcein and ABCG2-mediated transport of pheophorbide A (PhA). The accumulation of calcein, a fluorescent product of a known ABCB1 substrate drug calcein-AM [64], was determined in ABCB1-overexpressing NCI-ADR-RES and MDR19-HEK293 cells, whereas the accumulation of PhA, a known fluorescent substrate of ABCG2 [48], was determined in ABCG2-overexpressing S1-M1-80 and R482-HEK293 cells. We found that LY3023414 (*shaded*, *solid lines*) at 40 μM inhibited ABCB1-mediated calcein-AM efflux in NCI-ADR-RES (Fig. 4A) and MDR19-HEK293 (Fig. 4B) cells, and ABCG2-mediated PhA efflux in S1-M1-80 (Fig. 4C) and R482-HEK293 (Fig. 4D) cells. Of note, LY3023414 (*shaded*, *solid lines*), tariquidar, or Ko143 (*dotted lines*) alone did not have any significant effect on the accumulation of calcein-AM or PhA in the drug-sensitive parental cell lines (Fig. 4A – D, *left panels*).

3.5. LY3023414 stimulates the ATPase activity of ABCB1 and ABCG2

Knowing that ABCB1- and ABCG2-mediated substrate transport is coupled to the stimulation of ATP hydrolysis [65–69], we examined the effect of LY3023414 on the vanadate (V_i)-sensitive ATPase activity of ABCB1 and ABCG2 using membrane vesicles isolated from High-Five cells expressing either human ABCB1 or ABCG2 protein as described in Materials and methods. We found that LY3023414 stimulated the ATPase activity of ABCB1 in a concentration-dependent manner (Fig. 5A), reaching a maximum stimulation of 157% of the basal value of 116.58 ± 12.50 nmole P_i/min/mg protein. LY3023414 also stimulated the V_i-sensitive ATPase activity of ABCG2, reaching a maximum stimulation of 128% of the basal value of 228.87 ± 6.97 nmole P_i/min/mg protein (Fig. 5B). The stimulatory effect of LY3023414 is significant as the p values are 0.00451558 for ABCB1 and 0.00200136 for ABCG2, respectively.

3.6. Docking of LY3023414 in the drug-binding pocket of ABCB1 and ABCG2

In order to gain insight into the interactions between LY3023414 and the substrate-binding domains within ABCB1 and ABCG2, the *in silico* molecular docking analysis of LY3023414 in the inward-open structure of human ABCB1 (PDBID:6QEX) [54] and ABCG2 (PDBID:5NJ3) [55] was performed. Analysis of the lowest energy docking poses revealed the predicted sites of interaction between LY3023414 and several hydrophobic and aromatic residues located within the transmembrane domains (TMDs) of ABCB1 and ABCG2. Such residues are highlighted in Fig. 6A and Fig. 6B for ABCB1 and ABCG2 respectively. When comparing the binding of LY302341 with the binding of taxol in ABCB1 (PDBID: 6qex) and estrone-3-sulfate, mitoxantrone, imatinib and SN38 with ABCG2 (PDBIDs: 6hco, 6xvi, 6xvh and 6xvj)[70], we identified many residues that were in common for interacting with the substrates. In the case of ABCB1 the residues that are in common include MET 69, PHE 336, ILE 340, TYR 953, PHE 983 and MET 986 whereas in the case of ABCG2 the common residues are LEU 405, PHE 431, PHE 432, THR 435, ASN 436,

PHE 439, SER 440, THR 542, ILE 543, VAL 546 and MET 549 from both or either monomer. Interestingly there were more residues in common for ligands and LY3022341 with ABCG2 than with taxol for ABCB1. This is probably due to the fact that the binding site of ABCG2 is narrower and more defined than the one for ABCB1 where the molecules have more flexibility to bind in different orientations.

4. Discussion

The novel PI3K/mTOR dual inhibitor LY3023414 demonstrated promising preclinical activity [57, 59, 71, 72], and has now being tested in multiple clinical trials [73, 74]. However, the risk of developing resistance to LY3023414 could potentially present a therapeutic challenge in the future. Smith et al. demonstrated that through inhibition of the PAM signaling pathway, LY3023414 induced G1 phase cell-cycle arrest and showed antiproliferative activity against a collection of 32 human cancer cell lines of various origin [57], in which we noticed that the human colon HT-29 cancer cell line was highly resistant to LY3023414. Knowing that HT-29 cancer cells express ABCG2 [75, 76] and that the overexpression of ABCG2 in cancer cells often leads to drug resistance, the results here implicated that LY3023414 may be actively transported by ABCG2. Moreover, results of a recent phase 2 study demonstrated that LY3023414 has only modest single-agent activity and a manageable safety profile in patients with heavily pretreated advanced endometrial cancer prospectively selected for tumors with activating PI3K pathway mutations [74]. Considering that the PI3K inhibitors pictilisib (GDC-0941) [28], apitolisib (GDC-0980) [77, 78], CUDC-907 [29] and PF-4989216 [30] are substrates of ABCG2 and/or ABCB1, it is not inconceivable that induced expression of ABCB1 and/or ABCG2 in endometrial cancer cells [79–83] could play a role in the reduced response to LY3023414.

It is worth noting that the intricate relationship between the PI3K/AKT signaling pathway and the MDR phenotype mediated by ABCB1 and ABCG2 in cancer cell lines has been studied extensively by independent groups [4] [84, 85]. For instance, the activation of AKT has been implicated to positively regulate the surface expression of ABCG2 [86–88]. The acidic microenvironment-induced overexpression of ABCG2 via the PI3K/AKT signaling pathway was found to contribute to the MDR phenotype in lung cancer cells [89]. Huang *et al.* demonstrated that the inactivation of PTEN up-regulates the expression of ABCG2 expression in adult acute leukemia through the PI3K/AKT pathway [90]. More recently, Chen et al. discovered that urate increased the expression of ABCG2 in HT-29 and Caco-2 cell lines via activating the TLR4-NLRP3 inflammasome and PI3K/AKT signaling pathway [91]. In addition, the reversal effect of PI3K/AKT signaling pathway inhibitors on MDR mediated by ABCB1 and/or ABCG2 in cancer cells has also been described. It was reported that through the inhibition of the PI3K/AKT signaling pathway, ZSTK474 inhibited the drug transport function and downregulated the protein expression of ABCB1 and ABCG2 [92], whereas PI103 [93], perifosine [94], and LY294002 [95] downregulated ABCB1 expression in sarcoma, breast cancer, and gastric cancer cells, respectively. The PI3K/mTOR dual inhibitor dactolisib reversed MDR mediated by ABCB1 and ABCG2 in multidrug-resistant acute myeloid leukemia (AML) cells [96] and mesothelioma cell lines [97], respectively. Similarly, Huang et al. demonstrated that cepharanthine reverses ABCB1-mediated multidrug resistance in human ovarian carcinoma cells by inhibiting the PI3K/AKT

signaling pathway [98]. Moreover, natural products timosaponin A [99] and osthole [100] could downregulate the expression of ABCB1 in myelogenous leukemia K562/ADM cells, and the grape seed proanthocyanidin extract [101] and epigallocatechin-3-gallate (EGCG) [102] could reverse MDR in ABCB1-overexpressing multidrug-resistant cancer cells by inhibiting the PI3K/AKT signaling pathway.

In the present study, we found that LY3023414 inhibited the proliferation of cancer cells from different origins with IC_{50} values ranging from approximately 20 – 90 nM, which are comparable to the values reported previously by Smith *et al.* [57]. However, we discovered that cancer cells overexpressing ABCB1 or ABCG2, as well as HEK293 cells with ectopic expression of human ABCB1 (MDR19-HEK293) or human ABCG2 (R482-HEK293) were also resistant to LY3023414 as compared to the parental HEK293 cells (Table 1). Moreover, the effect of LY3023414 on PI3K signaling and G0/G1 cell-cycle arrest was significantly reduced in ABCB1-overexpressing NCI-ADR-RES and ABCG2-overexpressing S1-M1-80 cancer cell lines in comparison to the respective parental cell lines (Fig. 2). Nevertheless, the long-term effect of LY3023414 treatment on the expression of ABCB1 and ABCG2 in cancer patients remains to be determined. Considering that ABCB1- and ABCG2-mediated resistance to LY3023414 may present a therapeutic problem in the future, we tested whether inhibition of ABCB1 and ABCG2 can overcome LY3023414 resistance in ABCB1- and ABCG2-overexpressing multidrug-resistant cancer cells, NCI-ADR-RES and S1-M1-80 cancer cells. We discovered that tariquidar and Ko143 significantly increased the intracellular accumulation of LY3023414 (Fig. 3) and subsequently restored the efficacy of LY3023414 to inhibit PI3K/AKT signaling (Fig. 2) and the proliferation of these multidrug-resistant cancer cells (Table 2). Although there is still no FDA-approved ABCB1 or ABCG2 inhibitor available, we have demonstrated in principle that the efficacy of LY3023414 in ABCB1- and ABCG2-overexpressing multidrug-resistant cancer cells can be restored by inhibiting the function of ABCB1 and ABCG2. The facts that LY3023414 inhibits the transport of calcein-AM mediated by ABCB1 and the transport of PhA mediated by ABCG2 (Fig. 4) and in addition it stimulates the ATPase activity of ABCB1 and ABCG2 (the results of Fig. 5) support the conclusion that LY3023414 is a substrate for ABCB1 and ABCG2. Furthermore, the *in silico* molecular docking analysis of LY3023414 with the inward-open structure of human ABCB1 (PDBID:6QEX) [54] and ABCG2 (PDBID:5NJ3) (Fig. 6) support the binding of LY3023414 to the substrate-binding pockets of human ABCB1 and ABCG2 and inhibition of the binding and transport of fluorescent substrates such as Calcein-AM and PhA. The schematic (Fig. 7) describes the proposed mechanism by which both transporters confer resistance to LY3023414 in cancer cells.

In summary, our study revealed that LY3023414 is a substrate for ABCB1 and ABCG2, implicating ABCB1 and ABCG2 may serve as a mechanism of resistance for LY3023414. Moreover, taking into account the impact of ABCB1 and ABCG2 on the absorption and distribution of therapeutic drugs [103], ABCB1- and ABCG2-mediated transport of LY3023414 may present a significant therapeutic challenge for clinicians in the future. Therefore, although there is no clinically approved treatment to date due to problems such as toxicities [104] and poor metabolic stability of inhibitors [105], further investigation is warranted to explore drug combination approaches that may have the potential to overcome ABCB1 and ABCG2-mediated resistance to LY3023414.

Acknowledgments

This work was supported by funds from the Ministry of Science and Technology of Taiwan (MOST-108-2320-B-182-035), Chang Gung Medical Research Program (BMRPC17 and CMRPD1J0281). SL and SVA were supported by the Intramural Research Program of the National Institutes of Health, National Cancer Institute, Center for Cancer Research.

Abbreviations:

MDR	multidrug resistance
ABC	ATP-binding cassette
PI3K	phosphatidylinositol 3-kinase
mTOR	mammalian target of rapamycin
Vi	sodium orthovanadate
RF	Resistance factor

References

[1]. Alzahrani AS. PI3K/Akt/mTOR inhibitors in cancer: At the bench and bedside. Seminars in cancer biology. 2019.

[2]. West KA, Castillo SS, Dennis PA. Activation of the PI3K/Akt pathway and chemotherapeutic resistance. Drug Resist Updat. 2002;5:234–48. [PubMed: 12531180]

[3]. McCubrey JA, Steelman LS, Abrams SL, Lee JT, Chang F, Bertrand FE, et al. Roles of the RAF/MEK/ERK and PI3K/PTEN/AKT pathways in malignant transformation and drug resistance. Adv Enzyme Regul. 2006;46:249–79. [PubMed: 16854453]

[4]. Bleau AM, Hambardzumyan D, Ozawa T, Fomchenko EI, Huse JT, Brennan CW, et al. PTEN/PI3K/Akt pathway regulates the side population phenotype and ABCG2 activity in glioma tumor stem-like cells. Cell Stem Cell. 2009;4:226–35. [PubMed: 19265662]

[5]. Burris HA 3rd. Overcoming acquired resistance to anticancer therapy: focus on the PI3K/AKT/mTOR pathway. Cancer Chemother Pharmacol. 2013;71:829–42. [PubMed: 23377372]

[6]. Dienstmann R, Rodon J, Serra V, Tabernero J. Picking the point of inhibition: a comparative review of PI3K/AKT/mTOR pathway inhibitors. Mol Cancer Ther. 2014;13:1021–31. [PubMed: 24748656]

[7]. Janku F, Yap TA, Meric-Bernstam F. Targeting the PI3K pathway in cancer: are we making headway? Nature reviews Clinical oncology. 2018;15:273–91.

[8]. Markham A. Alpelisib: First Global Approval. Drugs. 2019;79:1249–53. [PubMed: 31256368]

[9]. Leroy C, Amante RJ, Bentires-Alj M. Anticipating mechanisms of resistance to PI3K inhibition in breast cancer: a challenge in the era of precision medicine. Biochem Soc Trans. 2014;42:733–41. [PubMed: 25109950]

[10]. Gottesman MM. Mechanisms of cancer drug resistance. Annual review of medicine. 2002;53:615–27.

[11]. Szakacs G, Paterson JK, Ludwig JA, Booth-Genthe C, Gottesman MM. Targeting multidrug resistance in cancer. Nature reviews. 2006;5:219–34.

[12]. Robey RW, Pluchino KM, Hall MD, Fojo AT, Bates SE, Gottesman MM. Revisiting the role of ABC transporters in multidrug-resistant cancer. Nat Rev Cancer. 2018;18:452–64. [PubMed: 29643473]

[13]. Gillet JP, Gottesman MM. Mechanisms of multidrug resistance in cancer. Methods Mol Biol. 2010;596:47–76. [PubMed: 19949920]

[14]. Szakacs G, Varadi A, Ozvegy-Laczka C, Sarkadi B. The role of ABC transporters in drug absorption, distribution, metabolism, excretion and toxicity (ADME-Tox). Drug discovery today. 2008;13:379–93. [PubMed: 18468555]

[15]. Gottesman M, Ambudkar SV. Overview: ABC transporters and human disease. J Bioenerg Biomembr. 2001;33:453–8. [PubMed: 11804186]

[16]. Paez JG, Janne PA, Lee JC, Tracy S, Greulich H, Gabriel S, et al. EGFR mutations in lung cancer: correlation with clinical response to gefitinib therapy. Science. 2004;304:1497–500. [PubMed: 15118125]

[17]. Agarwal S, Sane R, Gallardo JL, Ohlfest JR, Elmquist WF. Distribution of gefitinib to the brain is limited by P-glycoprotein (ABCB1) and breast cancer resistance protein (ABCG2)-mediated active efflux. J Pharmacol Exp Ther. 2010;334:147–55. [PubMed: 20421331]

[18]. Kim M, Laramy JK, Mohammad AS, Talele S, Fisher J, Sarkaria JN, et al. Brain Distribution of a Panel of Epidermal Growth Factor Receptor Inhibitors Using Cassette Dosing in Wild-Type and Abcb1/Abcg2-Deficient Mice. Drug Metab Dispos. 2019;47:393–404. [PubMed: 30705084]

[19]. van Hoppe S, Jamalpoor A, Rood JJM, Wagenaar E, Sparidans RW, Beijnen JH, et al. Brain accumulation of osimertinib and its active metabolite AZ5104 is restricted by ABCB1 (P-glycoprotein) and ABCG2 (breast cancer resistance protein). Pharmacol Res. 2019;146:104297. [PubMed: 31175939]

[20]. Wang T, Agarwal S, Elmquist WF. Brain distribution of cediranib is limited by active efflux at the blood-brain barrier. J Pharmacol Exp Ther. 2012;341:386–95. [PubMed: 22323823]

[21]. Mittapalli RK, Vaidhyanathan S, Sane R, Elmquist WF. Impact of P-glycoprotein (ABCB1) and breast cancer resistance protein (ABCG2) on the brain distribution of a novel BRAF inhibitor: vemurafenib (PLX4032). J Pharmacol Exp Ther. 2012;342:33–40. [PubMed: 22454535]

[22]. Wu CP, Sim HM, Huang YH, Liu YC, Hsiao SH, Cheng HW, et al. Overexpression of ATP-binding cassette transporter ABCG2 as a potential mechanism of acquired resistance to vemurafenib in BRAF(V600E) mutant cancer cells. Biochem Pharmacol. 2013;85:325–34. [PubMed: 23153455]

[23]. Wang J, Gan C, Sparidans RW, Wagenaar E, van Hoppe S, Beijnen JH, et al. P-glycoprotein (MDR1/ABCB1) and Breast Cancer Resistance Protein (BCRP/ABCG2) affect brain accumulation and intestinal disposition of encorafenib in mice. Pharmacol Res. 2018;129:414–23. [PubMed: 29155017]

[24]. Gampa G, Kim M, Mohammad AS, Parrish KE, Mladek AC, Sarkaria JN, et al. Brain Distribution and Active Efflux of Three panRAF Inhibitors: Considerations in the Treatment of Melanoma Brain Metastases. J Pharmacol Exp Ther. 2019;368:446–61. [PubMed: 30622172]

[25]. Parrish KE, Cen L, Murray J, Calligaris D, Kizilbash S, Mittapalli RK, et al. Efficacy of PARP Inhibitor Rucaparib in Orthotopic Glioblastoma Xenografts Is Limited by Ineffective Drug Penetration into the Central Nervous System. Mol Cancer Ther. 2015;14:2735–43. [PubMed: 26438157]

[26]. Durmus S, Sparidans RW, van Esch A, Wagenaar E, Beijnen JH, Schinkel AH. Breast cancer resistance protein (BCRP/ABCG2) and P-glycoprotein (P-GP/ABCB1) restrict oral availability and brain accumulation of the PARP inhibitor rucaparib (AG-014699). Pharm Res. 2015;32:37–46. [PubMed: 24962512]

[27]. de Gooijer MC, Buil LCM, Citirikkaya CH, Hermans J, Beijnen JH, van Tellingen O. ABCB1 Attenuates the Brain Penetration of the PARP Inhibitor AZD2461. Mol Pharm. 2018;15:5236–43. [PubMed: 30252484]

[28]. Salphati L, Lee LB, Pang J, Plise EG, Zhang X. Role of P-glycoprotein and breast cancer resistance protein-1 in the brain penetration and brain pharmacodynamic activity of the novel phosphatidylinositol 3-kinase inhibitor GDC-0941. Drug Metab Dispos. 2010;38:1422–6. [PubMed: 20522663]

[29]. Wu CP, Hsieh YJ, Hsiao SH, Su CY, Li YQ, Huang YH, et al. Human ATP-Binding Cassette Transporter ABCG2 Confers Resistance to CUDC-907, a Dual Inhibitor of Histone Deacetylase and Phosphatidylinositol 3-Kinase. Mol Pharm. 2016;13:784–94. [PubMed: 26796063]

[30]. Wu CP, Murakami M, Hsiao SH, Chou AW, Li YQ, Huang YH, et al. Overexpression of ATP-Binding Cassette Subfamily G Member 2 Confers Resistance to Phosphatidylinositol 3-Kinase Inhibitor PF-4989216 in Cancer Cells. Mol Pharm. 2017;14:2368–77. [PubMed: 28597653]

[31]. Hofmeister CC, Yang X, Pichiorri F, Chen P, Rozewski DM, Johnson AJ, et al. Phase I trial of lenalidomide and CCI-779 in patients with relapsed multiple myeloma: evidence for lenalidomide-CCI-779 interaction via P-glycoprotein. J Clin Oncol. 2011;29:3427–34. [PubMed: 21825263]

[32]. Tang SC, Sparidans RW, Cheung KL, Fukami T, Durmus S, Wagenaar E, et al. P-glycoprotein, CYP3A, and plasma carboxylesterase determine brain and blood disposition of the mTOR Inhibitor everolimus (Afinitor) in mice. Clin Cancer Res. 2014;20:3133–45. [PubMed: 24727322]

[33]. Beebe J, Zhang JT. CC-115, a Dual Mammalian Target of Rapamycin/DNA-Dependent Protein Kinase Inhibitor in Clinical Trial, Is a Substrate of ATP-Binding Cassette G2, a Risk Factor for CC-115 Resistance. J Pharmacol Exp Ther. 2019;371:320–6. [PubMed: 31455631]

[34]. Roschke AV, Tonon G, Gehlhaus KS, McTyre N, Bussey KJ, Lababidi S, et al. Karyotypic complexity of the NCI-60 drug-screening panel. Cancer Res. 2003;63:8634–47. [PubMed: 14695175]

[35]. Shen DW, Cardarelli C, Hwang J, Cornwell M, Richert N, Ishii S, et al. Multiple drug-resistant human KB carcinoma cells independently selected for high-level resistance to colchicine, adriamycin, or vinblastine show changes in expression of specific proteins. J Biol Chem. 1986;261:7762–70. [PubMed: 3711108]

[36]. Robey RW, Shukla S, Finley EM, Oldham RK, Barnett D, Ambudkar SV, et al. Inhibition of P-glycoprotein (ABCB1)- and multidrug resistance-associated protein 1 (ABCC1)-mediated transport by the orally administered inhibitor, CBT-1((R)). Biochem Pharmacol. 2008;75:1302–12. [PubMed: 18234154]

[37]. Robey RW, Honjo Y, Morisaki K, Nadjem TA, Runge S, Risbood M, et al. Mutations at amino-acid 482 in the ABCG2 gene affect substrate and antagonist specificity. Br J Cancer. 2003;89:1971–8. [PubMed: 14612912]

[38]. Miyake K, Mickley L, Litman T, Zhan Z, Robey R, Cristensen B, et al. Molecular cloning of cDNAs which are highly overexpressed in mitoxantrone-resistant cells: demonstration of homology to ABC transport genes. Cancer Res. 1999;59:8–13. [PubMed: 9892175]

[39]. Henrich CJ, Robey RW, Bokesch HR, Bates SE, Shukla S, Ambudkar SV, et al. New inhibitors of ABCG2 identified by high-throughput screening. Molecular cancer therapeutics. 2007;6:3271–8. [PubMed: 18089721]

[40]. Shen DW, Fojo A, Chin JE, Roninson IB, Richert N, Pastan I, et al. Human multidrug-resistant cell lines: increased mdr1 expression can precede gene amplification. Science. 1986;232:643–5. [PubMed: 3457471]

[41]. Henrich CJ, Bokesch HR, Dean M, Bates SE, Robey RW, Goncharova EI, et al. A high-throughput cell-based assay for inhibitors of ABCG2 activity. Journal of biomolecular screening. 2006;11:176–83. [PubMed: 16490770]

[42]. Wu CP, Shukla S, Calcagno AM, Hall MD, Gottesman MM, Ambudkar SV. Evidence for dual mode of action of a thiosemicarbazone, NSC73306: a potent substrate of the multidrug resistance linked ABCG2 transporter. Mol Cancer Ther. 2007;6:3287–96. [PubMed: 18089722]

[43]. Wu CP, Lusvarghi S, Wang JC, Hsiao SH, Huang YH, Hung TH, et al. Avapritinib: A Selective Inhibitor of KIT and PDGFRalpha that Reverses ABCB1 and ABCG2-Mediated Multidrug Resistance in Cancer Cell Lines. Mol Pharm. 2019;16:3040–52. [PubMed: 31117741]

[44]. Wu CP, Hsiao SH, Su CY, Luo SY, Li YQ, Huang YH, et al. Human ATP-Binding Cassette transporters ABCB1 and ABCG2 confer resistance to CUDC-101, a multi-acting inhibitor of histone deacetylase, epidermal growth factor receptor and human epidermal growth factor receptor 2. Biochem Pharmacol. 2014;92:567–76. [PubMed: 25450670]

[45]. Wu CP, Hsiao SH, Sim HM, Luo SY, Tuo WC, Cheng HW, et al. Human ABCB1 (P-glycoprotein) and ABCG2 mediate resistance to BI 2536, a potent and selective inhibitor of Polo-like kinase 1. Biochem Pharmacol. 2013;86:904–13. [PubMed: 23962445]

[46]. Wu CP, Hsieh YJ, Murakami M, Vahedi S, Hsiao SH, Yeh N, et al. Human ATP-binding cassette transporters ABCB1 and ABCG2 confer resistance to histone deacetylase 6 inhibitor ricolinostat (ACY-1215) in cancer cell lines. Biochem Pharmacol. 2018;155:316–25. [PubMed: 30028995]

[47]. Gribar JJ, Ramachandra M, Hrycyna CA, Dey S, Ambudkar SV. Functional characterization of glycosylation-deficient human P-glycoprotein using a vaccinia virus expression system. J Membr Biol. 2000;173:203–14. [PubMed: 10667916]

[48]. Robey RW, Steadman K, Polgar O, Morisaki K, Blayney M, Mistry P, et al. Pheophorbide a is a specific probe for ABCG2 function and inhibition. Cancer Res. 2004;64:1242–6. [PubMed: 14973080]

[49]. Ambudkar SV. Drug-stimulatable ATPase activity in crude membranes of human MDR1-transfected mammalian cells. Methods Enzymol. 1998;292:504–14. [PubMed: 9711578]

[50]. Ramachandra M, Ambudkar SV, Chen D, Hrycyna CA, Dey S, Gottesman MM, et al. Human P-glycoprotein exhibits reduced affinity for substrates during a catalytic transition state. Biochemistry. 1998;37:5010–9. [PubMed: 9538020]

[51]. Kerr KM, Sauna ZE, Ambudkar SV. Correlation between steady-state ATP hydrolysis and vanadate-induced ADP trapping in Human P-glycoprotein. Evidence for ADP release as the rate-limiting step in the catalytic cycle and its modulation by substrates. J Biol Chem. 2001;276:8657–64. [PubMed: 11121420]

[52]. Nandigama K, Lusvarghi S, Shukla S, Ambudkar SV. Large-scale purification of functional human P-glycoprotein (ABCB1). Protein expression and purification. 2019;159:60–8. [PubMed: 30851394]

[53]. Trott O, Olson AJ. AutoDock Vina: improving the speed and accuracy of docking with a new scoring function, efficient optimization, and multithreading. Journal of computational chemistry. 2010;31:455–61. [PubMed: 19499576]

[54]. Alam A, Kowal J, Broude E, Roninson I, Locher KP. Structural insight into substrate and inhibitor discrimination by human P-glycoprotein. Science. 2019;363:753–6. [PubMed: 30765569]

[55]. Taylor NMI, Manolaridis I, Jackson SM, Kowal J, Stahlberg H, Locher KP. Structure of the human multidrug transporter ABCG2. Nature. 2017;546:504–9. [PubMed: 28554189]

[56]. Wu CP, Lusvarghi S, Wang JC, Hsiao SH, Huang YH, Hung TH, et al. The Selective Class IIa Histone Deacetylase Inhibitor TMP195 Resensitizes ABCB1- and ABCG2-Overexpressing Multidrug-Resistant Cancer Cells to Cytotoxic Anticancer Drugs. International journal of molecular sciences. 2019;21.

[57]. Smith MC, Mader MM, Cook JA, Iversen P, Ajamie R, Perkins E, et al. Characterization of LY3023414, a Novel PI3K/mTOR Dual Inhibitor Eliciting Transient Target Modulation to Impede Tumor Growth. Mol Cancer Ther. 2016;15:2344–56. [PubMed: 27439478]

[58]. Zou Y, Ge M, Wang X. Targeting PI3K-AKT-mTOR by LY3023414 inhibits human skin squamous cell carcinoma cell growth in vitro and in vivo. Biochemical and biophysical research communications. 2017;490:385–92. [PubMed: 28623128]

[59]. Foley TM, Payne SN, Pasch CA, Yueh AE, Van De Hey DR, Korkos DP, et al. Dual PI3K/mTOR Inhibition in Colorectal Cancers with APC and PIK3CA Mutations. Molecular cancer research : MCR. 2017;15:317–27. [PubMed: 28184015]

[60]. Wallin JJ, Edgar KA, Guan J, Berry M, Prior WW, Lee L, et al. GDC-0980 is a novel class I PI3K/mTOR kinase inhibitor with robust activity in cancer models driven by the PI3K pathway. Mol Cancer Ther. 2011;10:2426–36. [PubMed: 21998291]

[61]. Dai CL, Tiwari AK, Wu CP, Su XD, Wang SR, Liu DG, et al. Lapatinib (Tykerb, GW572016) reverses multidrug resistance in cancer cells by inhibiting the activity of ATP-binding cassette subfamily B member 1 and G member 2. Cancer Res. 2008;68:7905–14. [PubMed: 18829547]

[62]. Sodani K, Tiwari AK, Singh S, Patel A, Xiao ZJ, Chen JJ, et al. GW583340 and GW2974, human EGFR and HER-2 inhibitors, reverse ABCG2- and ABCB1-mediated drug resistance. Biochem Pharmacol. 2012;83:1613–22. [PubMed: 22414725]

[63]. Kuang YH, Patel JP, Sodani K, Wu CP, Liao LQ, Patel A, et al. OSI-930 analogues as novel reversal agents for ABCG2-mediated multidrug resistance. Biochem Pharmacol. 2012;84:766–74. [PubMed: 22750060]

[64]. Hollo Z, Homolya L, Davis CW, Sarkadi B. Calcein accumulation as a fluorometric functional assay of the multidrug transporter. Biochimica et biophysica acta. 1994;1191:384–8. [PubMed: 7909692]

[65]. Ambudkar SV, Dey S, Hrycyna CA, Ramachandra M, Pastan I, Gottesman MM. Biochemical, cellular, and pharmacological aspects of the multidrug transporter. Annual review of pharmacology and toxicology. 1999;39:361–98.

[66]. Ozvegy C, Litman T, Szakacs G, Nagy Z, Bates S, Varadi A, et al. Functional characterization of the human multidrug transporter, ABCG2, expressed in insect cells. Biochemical and biophysical research communications. 2001;285:111–7. [PubMed: 11437380]

[67]. Ambudkar SV, Kimchi-Sarfaty C, Sauna ZE, Gottesman MM. P-glycoprotein: from genomics to mechanism. Oncogene. 2003;22:7468–85. [PubMed: 14576852]

[68]. Ambudkar SV, Cardarelli CO, Pashinsky I, Stein WD. Relation between the turnover number for vinblastine transport and for vinblastine-stimulated ATP hydrolysis by human P-glycoprotein. J Biol Chem. 1997;272:21160–6. [PubMed: 9261121]

[69]. Ludwig JA, Szakacs G, Martin SE, Chu BF, Cardarelli C, Sauna ZE, et al. Selective toxicity of NSC73306 in MDR1-positive cells as a new strategy to circumvent multidrug resistance in cancer. Cancer Res. 2006;66:4808–15. [PubMed: 16651436]

[70]. Orlando BJ, Liao M. ABCG2 transports anticancer drugs via a closed-to-open switch. Nature communications. 2020;11:2264.

[71]. Zaidi AH, Kosovec JE, Matsui D, Omstead AN, Raj M, Rao RR, et al. PI3K/mTOR Dual Inhibitor, LY3023414, Demonstrates Potent Antitumor Efficacy Against Esophageal Adenocarcinoma in a Rat Model. Annals of surgery. 2017;266:91–8. [PubMed: 27471841]

[72]. Sakamoto Y, Yamagishi S, Tanizawa Y, Tajimi M, Okusaka T, Ojima H. PI3K-mTOR pathway identified as a potential therapeutic target in biliary tract cancer using a newly established patient-derived cell panel assay. Japanese journal of clinical oncology. 2018;48:396–9. [PubMed: 29474549]

[73]. Bendell JC, Varghese AM, Hyman DM, Bauer TM, Pant S, Callies S, et al. A First-in-Human Phase 1 Study of LY3023414, an Oral PI3K/mTOR Dual Inhibitor, in Patients with Advanced Cancer. Clin Cancer Res. 2018;24:3253–62. [PubMed: 29636360]

[74]. Rubinstein MM, Hyman DM, Caird I, Won H, Soldan K, Seier K, et al. Phase 2 study of LY3023414 in patients with advanced endometrial cancer harboring activating mutations in the PI3K pathway. Cancer. 2020;126:1274–82. [PubMed: 31880826]

[75]. Kim JH, Park JM, Roh YJ, Kim IW, Hasan T, Choi MG. Enhanced efficacy of photodynamic therapy by inhibiting ABCG2 in colon cancers. BMC Cancer. 2015;15:504. [PubMed: 26149077]

[76]. Nie S, Huang Y, Shi M, Qian X, Li H, Peng C, et al. Protective role of ABCG2 against oxidative stress in colorectal cancer and its potential underlying mechanism. Oncology reports. 2018;40:2137–46. [PubMed: 30066914]

[77]. Salphati L, Pang J, Plise EG, Lee LB, Olivero AG, Prior WW, et al. Preclinical assessment of the absorption and disposition of the phosphatidylinositol 3-kinase/mammalian target of rapamycin inhibitor GDC-0980 and prediction of its pharmacokinetics and efficacy in human. Drug Metab Dispos. 2012;40:1785–96. [PubMed: 22696419]

[78]. Becker CM, Oberoi RK, McFarren SJ, Muldoon DM, Pafundi DH, Pokorny JL, et al. Decreased affinity for efflux transporters increases brain penetrance and molecular targeting of a PI3K/mTOR inhibitor in a mouse model of glioblastoma. Neuro Oncol. 2015;17:1210–9. [PubMed: 25972455]

[79]. Esteller M, Martinez-Palones JM, Garcia A, Xercavins J, Reventos J. High rate of MDR-1 and heterogeneous pattern of MRP expression without gene amplification in endometrial cancer. Int J Cancer. 1995;63:798–803. [PubMed: 8847137]

[80]. Esteller M, Xercavins J, Reventos J. Advances in the molecular genetics of endometrial cancer (Review). Oncology reports. 1999;6:1377–82. [PubMed: 10523715]

[81]. Hasegawa K, Ishikawa K, Kawai S, Torii Y, Kawamura K, Kato R, et al. Overcoming paclitaxel resistance in uterine endometrial cancer using a COX-2 inhibitor. Oncology reports. 2013;30:2937–44. [PubMed: 24100466]

[82]. Yamaguchi T, Kurita T, Nishio K, Tsukada J, Hachisuga T, Morimoto Y, et al. Expression of BAF57 in ovarian cancer cells and drug sensitivity. Cancer science. 2015;106:359–66. [PubMed: 25611552]

[83]. Yaguchi T, Onishi T. Estrogen induces cell proliferation by promoting ABCG2-mediated efflux in endometrial cancer cells. Biochemistry and biophysics reports. 2018;16:74–8. [PubMed: 30377671]

[84]. Pick A, Wiese M. Tyrosine kinase inhibitors influence ABCG2 expression in EGFR-positive MDCK BCRP cells via the PI3K/Akt signaling pathway. ChemMedChem. 2012;7:650–62. [PubMed: 22354538]

[85]. Wang L, Lin N, Li Y. The PI3K/AKT signaling pathway regulates ABCG2 expression and confers resistance to chemotherapy in human multiple myeloma. Oncology reports. 2019;41:1678–90. [PubMed: 30664164]

[86]. Mogi M, Yang J, Lambert JF, Colvin GA, Shiojima I, Skurk C, et al. Akt signaling regulates side population cell phenotype via Bcrp1 translocation. J Biol Chem. 2003;278:39068–75. [PubMed: 12851395]

[87]. Takada T, Suzuki H, Gotoh Y, Sugiyama Y. Regulation of the cell surface expression of human BCRP/ABCG2 by the phosphorylation state of Akt in polarized cells. Drug Metab Dispos. 2005;33:905–9. [PubMed: 15843490]

[88]. Hu C, Li H, Li J, Zhu Z, Yin S, Hao X, et al. Analysis of ABCG2 expression and side population identifies intrinsic drug efflux in the HCC cell line MHCC-97L and its modulation by Akt signaling. Carcinogenesis. 2008;29:2289–97. [PubMed: 18820285]

[89]. Hu CF, Huang YY, Wang YJ, Gao FG. Upregulation of ABCG2 via the PI3K-Akt pathway contributes to acidic microenvironment-induced cisplatin resistance in A549 and LTEP-a-2 lung cancer cells. Oncology reports. 2016;36:455–61. [PubMed: 27221310]

[90]. Huang FF, Wu DS, Zhang L, Yu YH, Yuan XY, Li WJ, et al. Inactivation of PTEN increases ABCG2 expression and the side population through the PI3K/Akt pathway in adult acute leukemia. Cancer Lett. 2013;336:96–105. [PubMed: 23603434]

[91]. Chen M, Lu X, Lu C, Shen N, Jiang Y, Chen M, et al. Soluble uric acid increases PDZK1 and ABCG2 expression in human intestinal cell lines via the TLR4-NLRP3 inflammasome and PI3K/Akt signaling pathway. Arthritis research & therapy. 2018;20:20. [PubMed: 29415757]

[92]. Muthiah D, Callaghan R. Dual effects of the PI3K inhibitor ZSTK474 on multidrug efflux pumps in resistant cancer cells. Eur J Pharmacol. 2017;815:127–37. [PubMed: 28912036]

[93]. Marklein D, Graab U, Naumann I, Yan T, Ridzewski R, Nitzki F, et al. PI3K inhibition enhances doxorubicin-induced apoptosis in sarcoma cells. PLoS One. 2012;7:e52898. [PubMed: 23300809]

[94]. Lin X, Zhang X, Wang Q, Li J, Zhang P, Zhao M, et al. Perifosine downregulates MDR1 gene expression and reverses multidrug-resistant phenotype by inhibiting PI3K/Akt/NF-kappaB signaling pathway in a human breast cancer cell line. Neoplasma. 2012;59:248–56. [PubMed: 22329846]

[95]. Xie X, Tang B, Zhou J, Gao Q, Zhang P. Inhibition of the PI3K/Akt pathway increases the chemosensitivity of gastric cancer to vincristine. Oncology reports. 2013;30:773–82. [PubMed: 23743572]

[96]. Deng L, Jiang L, Lin XH, Tseng KF, Liu Y, Zhang X, et al. The PI3K/mTOR dual inhibitor BEZ235 suppresses proliferation and migration and reverses multidrug resistance in acute myeloid leukemia. Acta pharmacologica Sinica. 2017;38:382–91. [PubMed: 28042875]

[97]. Fischer B, Frei C, Moura U, Stahel R, Felley-Bosco E. Inhibition of phosphoinositide-3 kinase pathway down regulates ABCG2 function and sensitizes malignant pleural mesothelioma to chemotherapy. Lung cancer. 2012;78:23–9. [PubMed: 22857894]

[98]. Huang CZ, Wang YF, Zhang Y, Peng YM, Liu YX, Ma F, et al. Cepharanthine hydrochloride reverses Pglycoprotein-mediated multidrug resistance in human ovarian carcinoma A2780/Taxol cells by inhibiting the PI3K/Akt signaling pathway. Oncology reports. 2017;38:2558–64. [PubMed: 28791369]

[99]. Chen JR, Jia XH, Wang H, Yi YJ, Wang JY, Li YJ. Timosaponin A-III reverses multi-drug resistance in human chronic myelogenous leukemia K562/ADM cells via downregulation of

MDR1 and MRP1 expression by inhibiting PI3K/Akt signaling pathway. Int J Oncol. 2016;48:2063–70. [PubMed: 26984633]

[100]. Wang H, Jia XH, Chen JR, Wang JY, Li YJ. Osthole shows the potential to overcome P-glycoproteinmediated multidrug resistance in human myelogenous leukemia K562/ADM cells by inhibiting the PI3K/Akt signaling pathway. Oncology reports. 2016;35:3659–68. [PubMed: 27109742]

[101]. Lin KN, Jiang YL, Zhang SG, Huang SY, Li H. Grape seed proanthocyanidin extract reverses multidrug resistance in HL-60/ADR cells via inhibition of the PI3K/Akt signaling pathway. Biomedicine & pharmacotherapy = Biomedecine & pharmacotherapie. 2020;125:109885. [PubMed: 32007917]

[102]. Satonaka H, Ishida K, Takai M, Koide R, Shigemasa R, Ueyama J, et al. (−)-Epigallocatechin-3-gallate Down-regulates Doxorubicin-induced Overexpression of P-glycoprotein Through the Coordinate Inhibition of PI3K/Akt and MEK/ERK Signaling Pathways. Anticancer research. 2017;37:6071–7. [PubMed: 29061787]

[103]. Shukla S, Ohnuma S, Ambudkar SV. Improving cancer chemotherapy with modulators of ABC drug transporters. Curr Drug Targets. 2011;12:621–30. [PubMed: 21039338]

[104]. Pusztai L, Wagner P, Ibrahim N, Rivera E, Theriault R, Booser D, et al. Phase II study of tariquidar, a selective P-glycoprotein inhibitor, in patients with chemotherapy-resistant, advanced breast carcinoma. Cancer. 2005;104:682–91. [PubMed: 15986399]

[105]. Liu K, Zhu J, Huang Y, Li C, Lu J, Sachar M, et al. Metabolism of KO143, an ABCG2 inhibitor. Drug Metab Pharmacokinet. 2017;32:193–200. [PubMed: 28619281]

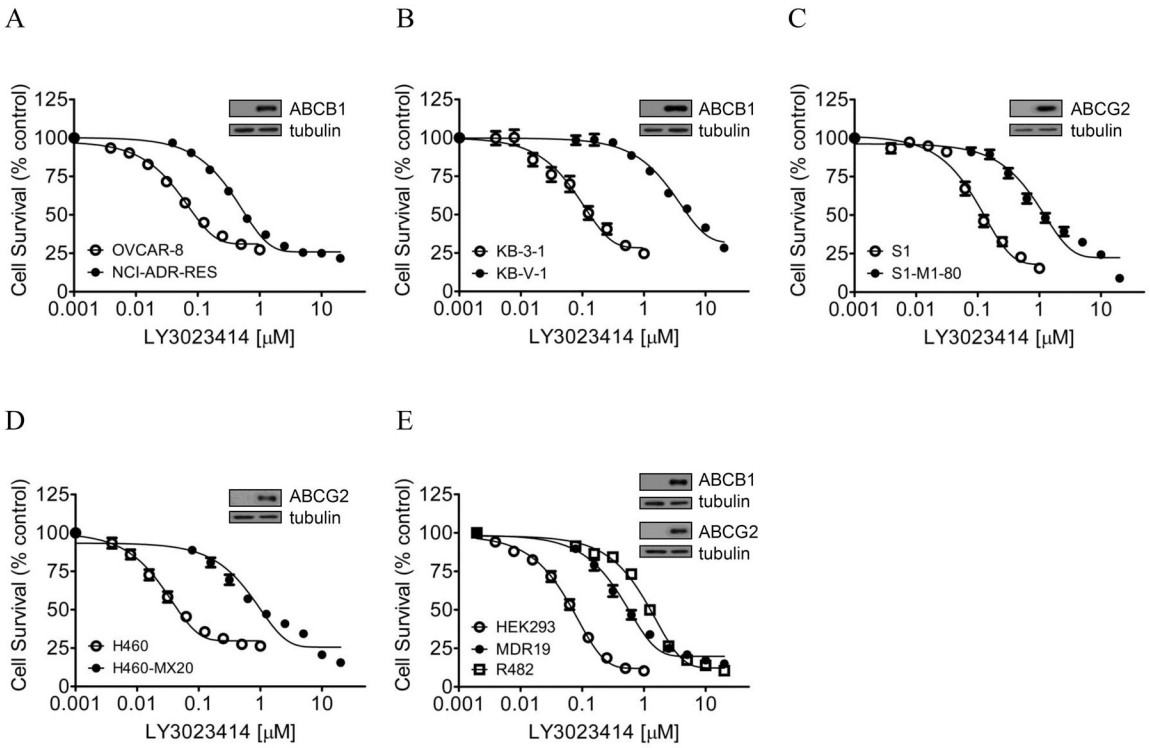

Fig. 1.

Differential cytotoxicity of LY3023414 in drug-sensitive cells and multidrug-resistant cells overexpressing either ABCB1 or ABCG2. The cytotoxicity of LY3023414 (final DMSO concentration 0.5% (v/v)) in (A) drug-sensitive human OVCAR ovarian cancer cell line (open circles) and its ABCB1-overexpressing variant NCI-ADR-RES (filled circles); (B) drug-sensitive human KB-3–1 epidermal cancer cell line (open circles) and its ABCB1-overexpressing KB-V-1 (filled circles); (C) drug-sensitive human S1 colon cancer cell line (open circles) and its ABCG2-overexpressing S1-M1-80 (filled circles); (D) drug-sensitive human H460 lung cell line (open circles) and its ABCG2-overexpressing H460-MX20 (filled circles); (E) parental pcDNA-HEK293 cells (open circles), HEK293 cells transfected with human ABCB1 (MDR19-HEK293, filled circles) and HEK293 cells transfected with human ABCG2 (R482-HEK293, open squares) was determined over a period of 72 h as described in Materials and methods. Representative immunoblots of ABCB1 and ABCG2 are shown in insets. Points, mean values from at least three independent experiments; bars, SEM.

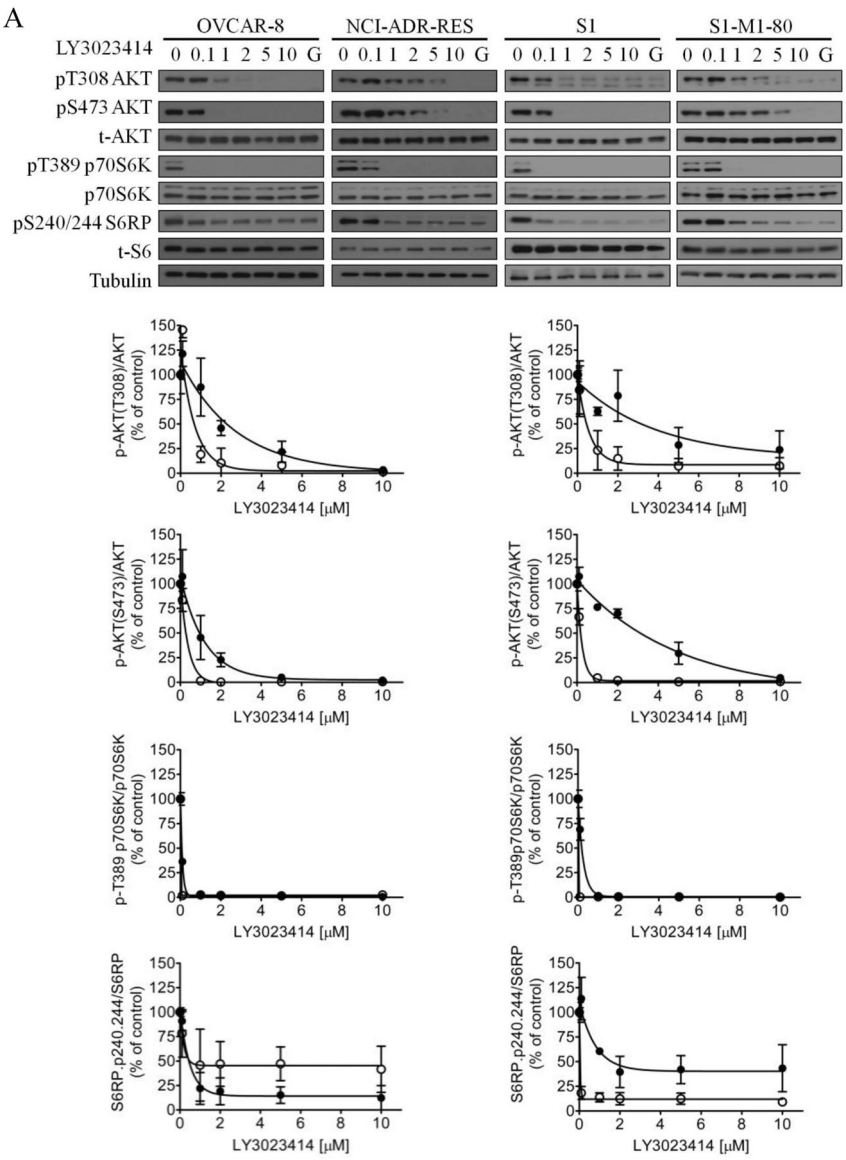

B

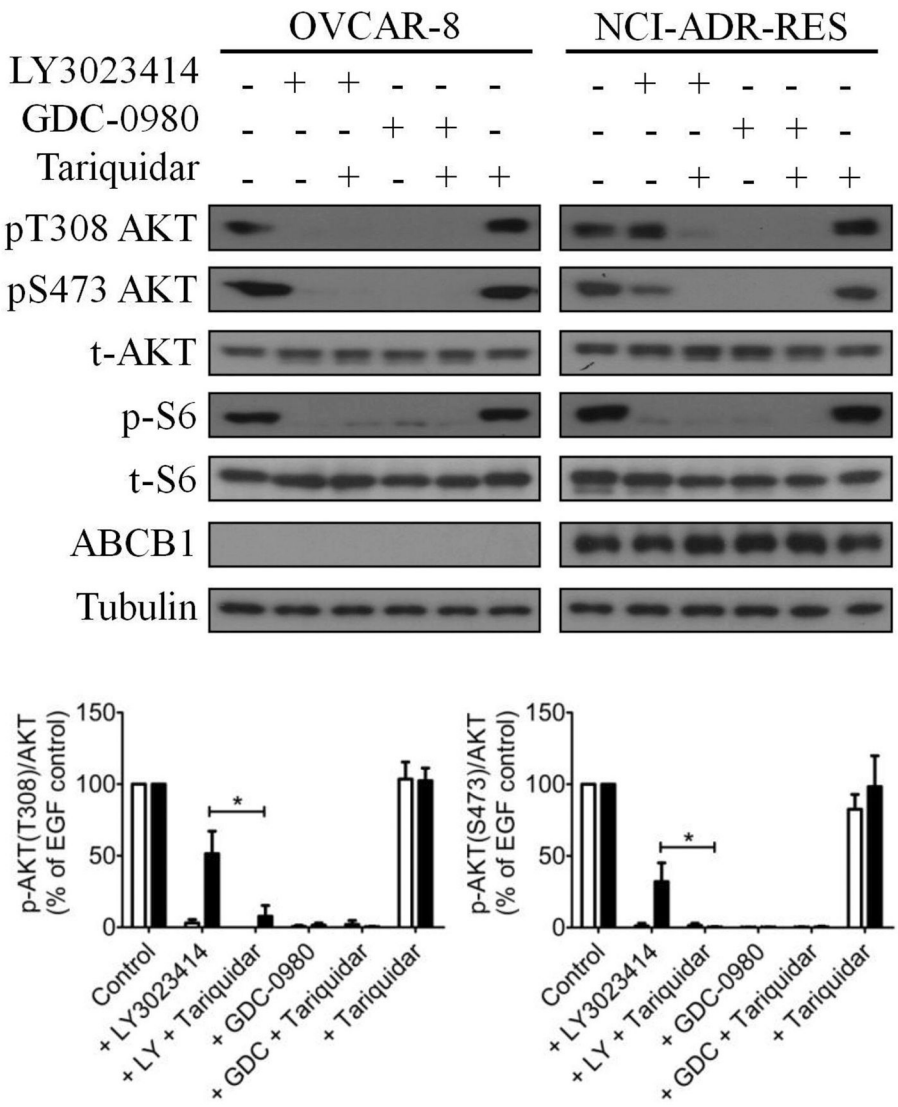

C

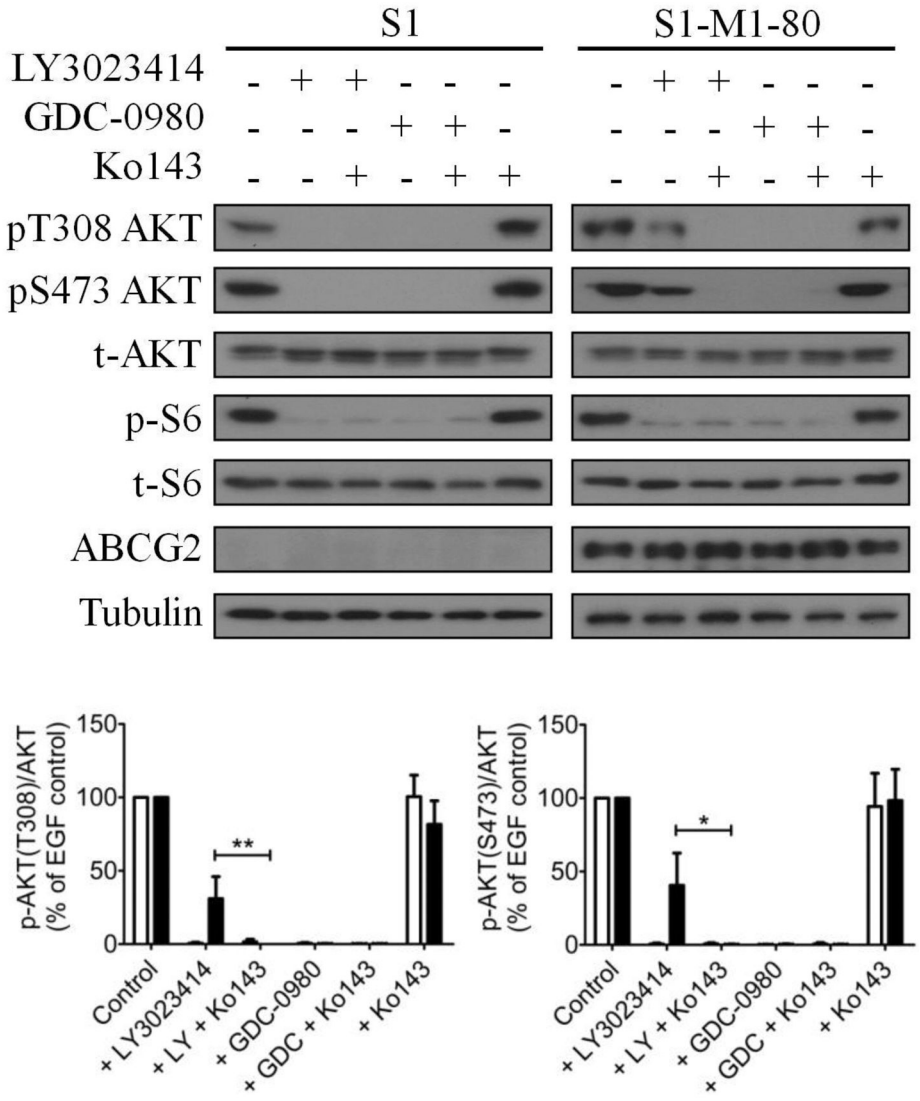

D

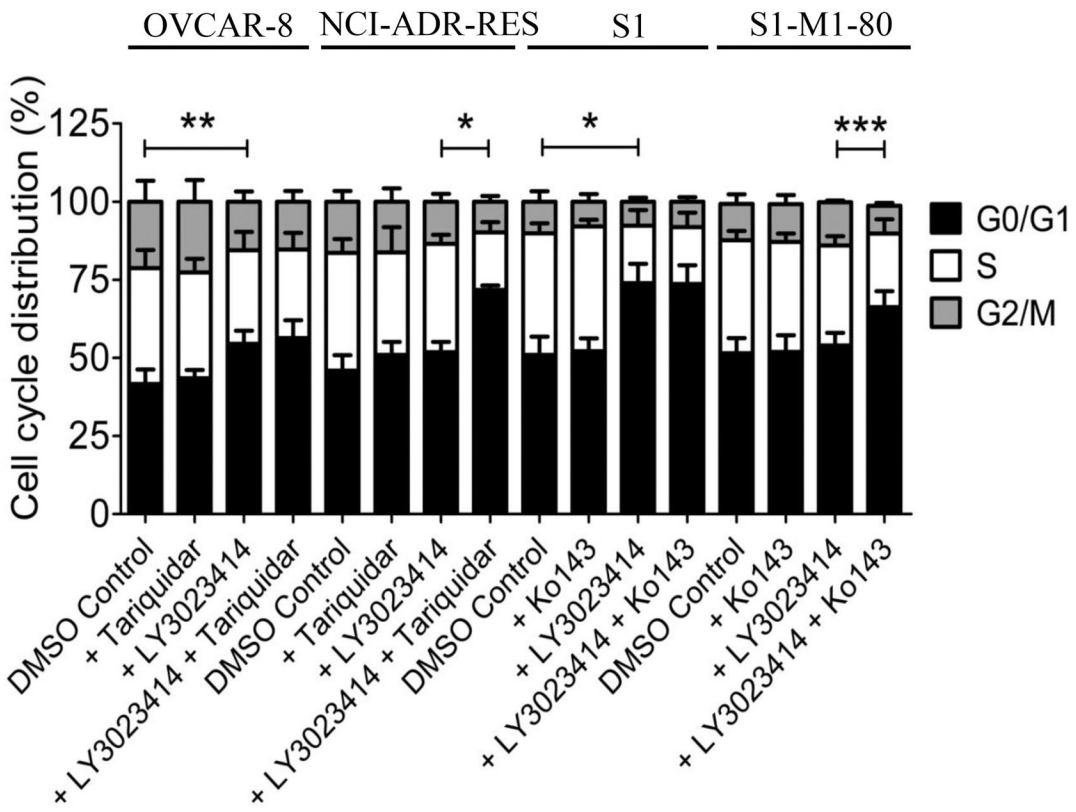

Fig. 2.

The effect of LY3023414 on PI3K/AKT/mTOR signaling pathway and G0/G1 cell cycle arrest in human cancer cell lines. (A) Representative immunoblot images (upper panels) and quantification of integrated intensity (lower panels) of phosphorylation of AKT at T308 (pT308 AKT) or S473 (pS473 AKT), total Akt (t-AKT), phosphorylation of p70 ribosomal protein S6 kinase (pT389 p70S6K), p70 ribosomal protein S6 kinase (p70S6K), ribosomal protein S6 phosphorylation (pS240/244 S6RP) and total S6 (t-S6), and tubulin of lysates from parental OVCAR-8 and multidrug-resistant NCI-ADR-RES cancer cells, as well as parental S1 and multidrug-resistant S1-M1-80 cancer cells treated with increasing concentrations (0 – 10 μM) of LY3023414 or 10 μM of a dual PI3K/mTOR inhibitor GDC-0980 (G). Representative immunoblot images (upper panels) and quantification of integrated intensity (lower panels) of pT308 AKT or pS473 AKT, t-Akt, ribosomal protein S6 phosphorylation (p-S6) and total S6 (t-S6), ABCB1, ABCG2 and tubulin of lysates from (B) OVCAR-8 and NCI-ADR-RES cells or (C) S1 and S1-M1-80 cells treated with DMSO (control), 2 μM of LY3023414 (+ LY) or 10 μM of a dual PI3K/mTOR inhibitor GDC-0980 (+ GDC) in the absence or presence of 1 μM of tariquidar or Ko143 in final DMSO concentration of 0.5% (v/v) as indicated for 2 h before processed for immunoblotting. Human EGF (50 ng/mL) was added to the culture medium for 5 min to stimulate phosphorylation. Quantification of relative levels of AKT phosphorylation in drug-sensitive

(*white bars*) and multidrug-resistant (*black bars*) cells, presented as mean ± S.D. calculated from more than three independent experiments. (D) OVCAR-8 and NCI-ADR-RES cells, as well as S1 and S1-M1-80 cells, were plated and treated with DMSO (control), 2 μM of LY3023414, 1 μM of tariquidar or 1 μM of Ko143 alone or in combination as indicated for 24 h before harvest for cell cycle analysis. Quantifications of cells in each of the cell cycle stages are shown as mean ± S.D. calculated from more than three independent experiments. *$p < 0.05$; **$p < 0.01$; ***$p < 0.001$, versus the same treatment in the absence of tariquidar or Ko143.

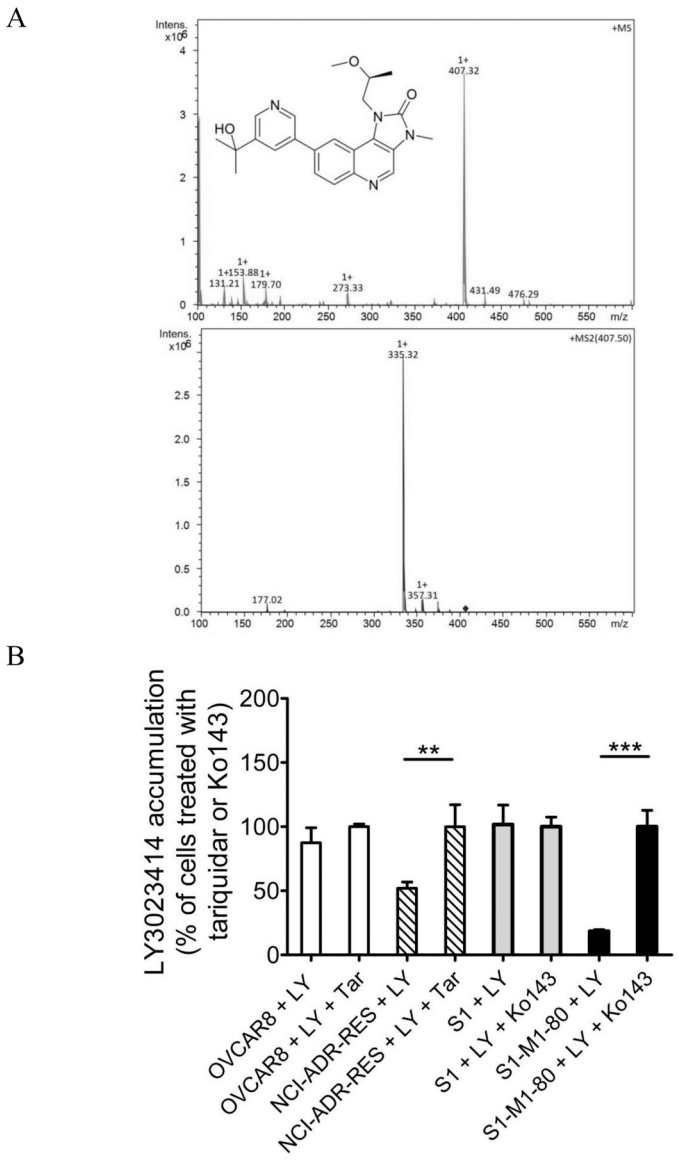

Fig. 3.

The intracellular accumulation of LY3023414 in cancer cells is reduced in cancer cells overexpressing ABCB1 or ABCG2. (A) The chemical structure and product ion mass spectra of LY3023414 with the expected fragments. (B) Quantification of intracellular LY3023414 by HPLC-MS/MS analysis in parental OVCAR-8 (white bars) and in ABCB1-overexpressing NCI-ADR-RES (striped bars) cells, as well as in parental S1 (grey bars) and ABCG2-overexpressing S1-M1-80 (black bars) cells. Cells were treated with 10 μM of LY3023414 in the presence or absence of 10 μM of tariquidar or Ko143 as indicated for 1 hour and processed as described in Materials and methods. Values are presented as mean values ± S.D. calculated from at least three independent experiments. $^{**}p < 0.01$; $^{***}p < 0.001$.

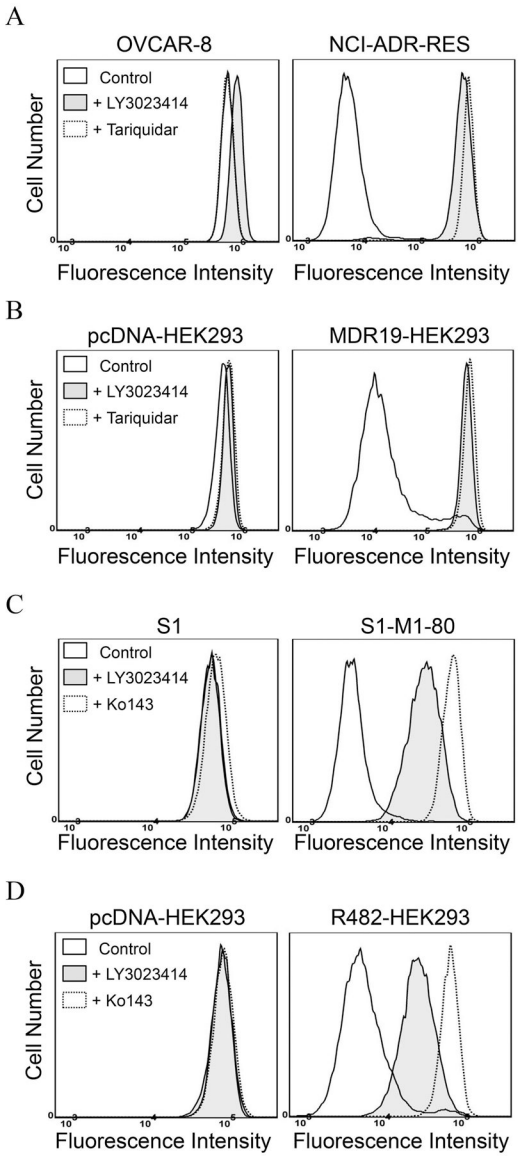

Fig. 4.

The effect of LY3023414 on the fluorescent drug transport mediated by ABCB1 and ABCG2. The accumulation of calcein in (A) OVCAR-8 and ABCB1-overexpressing NCI-ADR-RES cells, and in (B) pcDNA-HEK293 and ABCB1-transfected MDR19-HEK293 cells, or the accumulation of pheophorbide A (PhA) in (C) S1 and ABCG2-overexpressing S1-M1-80 cells, and in (D) pcDNA-HEK293 and ABCG2-transfected R482-HEK293 cells, were measured in the presence of DMSO (solid lines) or 40 μM of LY3023414 (shaded, solid lines) or 1 μM of tariquidar or Ko143 (dotted lines), and analyzed immediately by flow cytometry. Representative histograms of three independent experiments are shown.

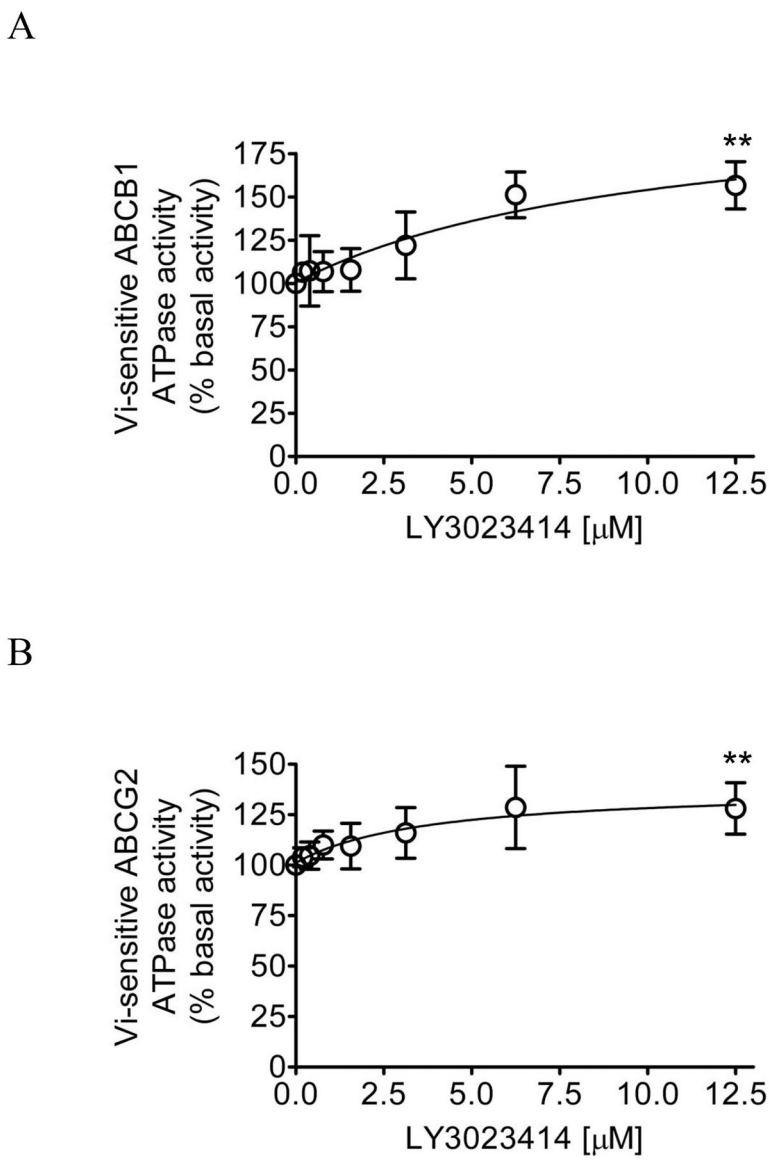

Fig. 5.

LY3023414 stimulates the ATPase activity of ABCB1 and ABCG2. The effect of LY3023414 (0 – 12.5 μM) on vanadate (V_i)-sensitive ATPase activity of (A) ABCB1 and (B) ABCG2 was determined by endpoint Pi assay, as described in Materials and methods. Data presented as mean ± SD. from three independent experiments. $^{**}p < 0.01$.

A

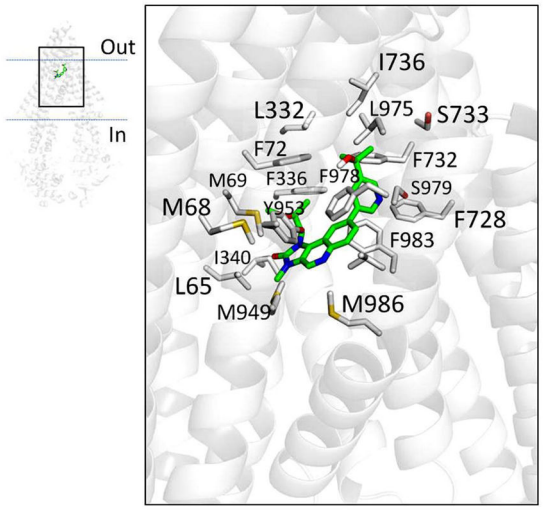

Pose	Docking score (kcal/mol)
1	-11.2
2	-10.5
3	-10.5
4	-10.4
5	-10.3
6	-10.3
7	-10.2
8	-10.2
9	-10.2

B

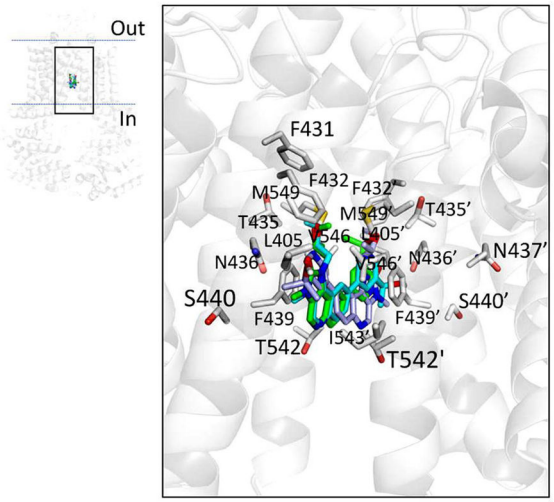

Pose	Docking score (kcal/mol)
1	-10.6
2	-10.6
3	-10.6
4	-10.4
5	-10.4
6	-10.4
7	-10.3
8	-10.2
9	-10.2

Fig. 6.

Binding of LY3023414 in the substrate-binding pockets of ABCB1 and ABCG2. LY3023414 was docked to the cryo-electron microscopy inward-open structure of (A) human ABCB1 (PDBID:6QEX) and (B) human ABCG2 (PDB: 5NJ3) using AutoDock Vina software as described in Materials and methods. LY3023414 lowest energy pose binding to ABCB1 is shown in green, whereas the three lowest energy poses of LY3023414 binding to ABCG2, all with the same docking score, are shown in green, cyan, and light blue. Residues that are within 5Å of the ligand are highlighted. The docking scores of the low-energy poses (tighter binding) of LY3023414 in the transmembrane region of ABCB1 and ABCG2 are presented on the right of each panel. Figures were prepared using the PyMOL molecular graphics system, Version 1.7 Shrödinger, LLC.

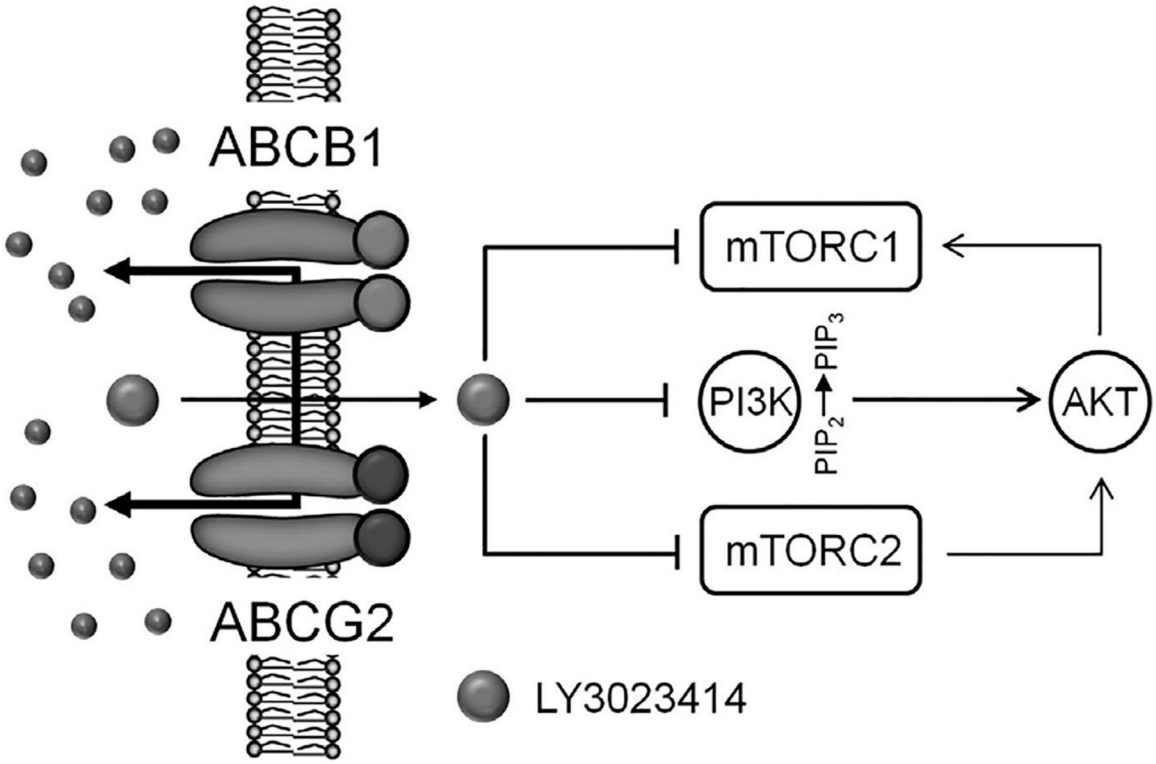

Fig. 7.

A schematic diagram illustrating the impact of ABCB1 and ABCG2 on the efficacy of LY3023414 in cancer cells. ABCB1- and ABCG2-mediated efflux of LY3023414 reduces the inhibition of PI3K and mTOR signaling, resulting in a continuous proliferation of cancer cells that express ABCB1 or ABCG2.

Table 1.

Cytotoxicity of LY3023414 in ABCB1- or ABCG2-overexpressing cell lines and respective parental cell lines.

Cell line	Type of carcinoma	Transporter expressed	IC_{50} (nM)[†]	R.F[‡]
OVCAR-8	ovarian	-	44.54 ± 2.20	1
NCI-ADR-RES	ovarian	ABCB1	337.46 ± 23.76***	8
KB-3–1	epidermal	-	67.20 ± 6.52	1.0
KB-V-1	epidermal	ABCB1	2467.20 ± 223.81***	37
S1	colon	-	84.39 ± 15.65	1.0
S1-M1-80	colon	ABCG2	1476.80 ± 246.91***	17
H460	lung	-	20.87 ± 0.68	1.0
H460-MX20	lung	ABCG2	852.16 ± 135.15***	41
pcDNA-HEK293	-	-	79.67 ± 7.17	1.0
MDR19-HEK293	-	ABCB1	821.05 ± 161.02**	10
R482-HEK293	-	ABCG2	988.77 ± 141.48***	12

Abbreviation: RF, resistance factor.

[†] IC_{50} values are mean ± SD calculated from dose-response curves obtained from at least three independent experiments using cytotoxicity assay as described in *Materials and methods*.

[‡] RF values were calculated by dividing IC_{50} value of LY3023414 in ABCB1- or ABCG2-expressing cells by IC_{50} value of LY3023414 in respective parental cells.

* $p < 0.05$;

** $p < 0.01$;

*** $p < 0.001$.

Table 2.

The effect of tariquidar and Ko143 on the cytotoxicity of LY3023414 in cells overexpressing ABCB1 or ABCG2.

Cell line	Mean IC_{50} ± SD [nM]†		
	LY3023414	LY3023414 + tariquidar	LY3023414 + Ko143
OVCAR-8	44.54 ± 2.20	50.87 ± 2.60*	N.D
NCI-ADR-RES	337.46 ± 23.76	52.71 ± 5.00***	N.D
S1	84.39 ± 15.65	N.D	136.31 ± 21.71*
S1-M1-80	1476.80 ± 246.91	N.D	176.98 ± 39.96***
pcDNA-HEK293	79.67 ± 7.17	85.05 ± 7.22	72.55 ± 7.14
MDR19-HEK293	821.05 ± 161.02	106.03 ± 24.82**	N.D
R482-HEK293	988.77 ± 141.48	N.D	144.85 ± 22.79***

Abbreviation: N.D, not determined.

† IC_{50} values are mean ± SD in the presence and absence of 1 μM tariquidar or 1 μM Ko143. The IC_{50} values were calculated from dose-response curves obtained from three independent experiments.

* $p < 0.05$;

** $p < 0.01$;

*** $p < 0.001$.